FEATURE ARTICLE

Conformational and Energetic Analysis of Saturated Organic Ring Compounds by 2 + 1 Resonance-Enhanced Multiphoton Ionization Spectroscopy

Alan R. Potts and Tomas Baer*

Department of Chemistry, University of North Carolina, Chapel Hill, North Carolina 27599-3290

Received: August 11, 1997; In Final Form: September 24, 1997[⊗]

The UV transition to the 3s Rydberg state in a number of saturated cyclic compounds has yielded a wealth of structural and energetic information. The HOMO → 3s spectra of pulsed molecular beam cooled samples can be conveniently investigated by 2 + 1 resonance-enhanced multiphoton ionization (REMPI) using pulsed laser light in the 360−420 nm region. The transition origins for a variety of methyl- and ethyl-substituted cyclohexanes, cyclohexanones, cyclopentanones, and tetrahyrdopyrans, as well as bicyclic compounds such as decalone and various camphors, are highly sensitive to the location of alkyl substitution as well as the orientation of the alkyl group (axial vs equatorial). In addition, the orientation of the ethyl rotor can be determined from the spectra. This technique is especially useful for investigating molecules in which several equilibrating conformations make the analysis of room-temperature spectra difficult. By rapid cooling in the molecular beam, higher energy conformers can be frozen out and investigated individually. By varying the temperature of the nozzle, it is possible to alter the conformational equilibria and to determine the $\Delta H°$ for the various structures. These studies demonstrate that, in many cases, the concentrations of the various conformations are cooled so rapidly that no equilibration of their populations is possible, even up to 150 °C. This shows that vibrational relaxation in the molecular beam is much more rapid than the conformer equilibration reaction.

Introduction

The determinations of molecular structures and energies are two of the most important tasks in physical chemistry. The major goal of all diffraction techniques and a large portion of spectroscopic work involves the elucidation of molecular structure. This task becomes particularly challenging when the molecules reside in various conformations separated by low interconversion barriers. Classic examples include the nearly planar five-membered saturated ring compounds such as substituted cyclopentanes, cyclopentanones, and tetrahydrofurans. At thermal energies, low-energy pseudorotation barriers permit rapid interconversion among the various twisted structures.[1−5] The UV spectra of a number of these have been analyzed in terms of two-dimensional potential energy surfaces in which two interacting vibrational modes result in complex vibrational structure.

Six-membered saturated cyclic compounds, which are most stable in the chair conformation, reside in slightly deeper potential wells and are thus somewhat easier to investigate. However, when groups such as ethyl and methoxy are substituted for hydrogen atoms on these rings, various rotor conformations are possible. These hindered rotor wells, which are separated by low barriers, not only affect the molecular structure; the accompanying low-frequency vibrations strongly influence the molecule's heat capacity.

A major difficulty in the investigation of rapidly interconverting or fluxional molecules in liquids and gases is related to the time scale of the interconversion process. If the spectroscopic technique is slow, such as NMR, then the spectrum contains information only about the average structure of all the conformations. This problem can be solved in some cases by reducing the sample temperature, thereby slowing the interconversion rates to the time scale of the experiment.[6,7] However, this is done at the expense of signal intensity for the higher energy conformer.

Another approach involves rapid cooling of the room temperature mixture of molecular conformations in a molecular beam. It is no exaggeration to state that the cooling of molecules in molecular beams has revolutionized visible and UV spectroscopy during the past 20 years. The combination of pulsed molecular beams and pulsed lasers is particularly powerful because this optimizes both the laser intensity and the sample density without requiring large experimental chambers and vacuum pumps.[8−11] The spectra of the cold samples are greatly simplified by the elimination of hot bands. In addition, it is possible to trap higher energy conformations so that the various structures of a molecule can be investigated by high-resolution spectroscopy.[12−29] A number of investigators have pursued the study of structural isomers by this approach in which the signal is monitored either by resonance-enhanced multiphoton ionization (REMPI) or by laser-induced fluorescence (LIF). In particular, the orientation of substituents such as OH, ethyl, and ethoxy on the benzene ring have been studied by these methods.[17,18,20,22,30−32]

We have investigated the structure of various configurational and conformational isomers of many saturated ring compounds (cyclohexanes, cyclopentanones, cyclohexanones, tetrahydrofurans (THF), and tetrahydropyrans (THP)) for a number of years.[28,29,33−45] These structures have the interesting feature that, in the chair conformation of the six-membered ring, substituents can be arranged in either axial or equatorial orientations.

[⊗] Abstract published in *Advance ACS Abstracts,* November 1, 1997.

S1089-5639(97)02616-9 CCC: $14.00

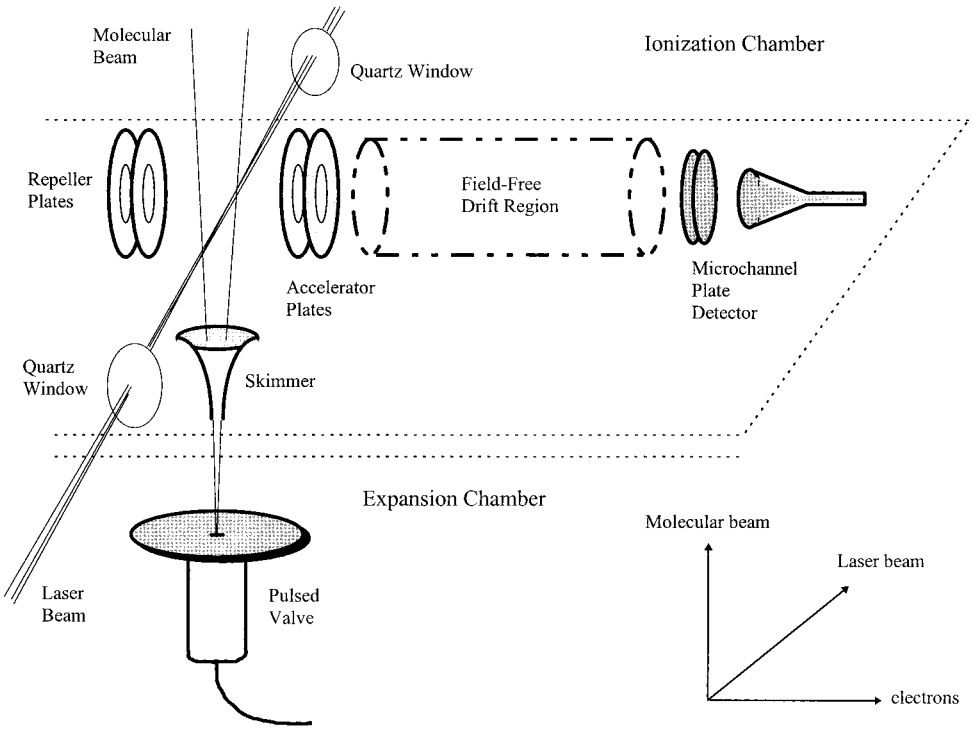

Figure 1. The experimental REMPI setup.

Furthermore, the ring can invert to a second chair conformation, thereby converting an axial to an equatorial substituent. A similar situation arises in the saturated five-membered ring system, but because of its near-planar structure, the substituents are pseudoaxial and pseudoequatorial.[46]

A particularly interesting and information-rich optical transition is the n → 3s Rydberg excitation which can be conveniently studied by 2 + 1 REMPI. The n → 3s transition is the first electronic transition for ethers and the second for ketones (the first being n → π^*). The analysis of these well-resolved spectra showed that methyl substitution at various locations and orientations (axial vs equatorial) with respect to the functional group results in predictable shifts of the transition origin. These single methyl group shifts, which were determined on the basis more than 60 mono-, di-, and trimethyl-substituted cyclic ketones, ethers, and cyclohexanones range from +400 to −750 cm^{-1} per methyl group.[42]

In addition to the correlation of the spectra to structural details, our experiments have made it possible to determine the relative enthalpies of the various conformations in the gas phase. This is of particular interest because the energetics of many conformations are not well-known. Most of the data are in the form of $\Delta G°$ values in the liquid phase. Because of the small entropy difference between conformations, $\Delta G°$ and $\Delta H°$ values differ slightly. Liquid- and gas-phase $\Delta H°$ values differ because of the different heats of vaporization of the two conformers. This is summarized by the following thermochemical diagram which relates the enthalpy difference between conformers A and B in the gas and liquid phases and their respective heats of vaporization.

$$\begin{array}{ccc} \text{A(gas)} & \longrightarrow & \text{B(gas)} \\ {\scriptstyle \Delta H_{vap}}\uparrow & & \downarrow{\scriptstyle \Delta H_{vap}} \\ \text{A(liq)} & \longrightarrow & \text{B(liq)} \end{array}$$

Although differences in ΔH_{vap} for conformers appear to be relatively small (ca. 0.1−0.2 kcal/mol), there are a number of molecules in which the $\Delta H°$ for the equilibrium between conformers is strongly influence by the solvent. In those cases, the heat of vaporization is very different for the two conformations.

In most saturated six-membered rings the equatorial is more stable than the axial orientation by 1−2 kcal/mol. The destabilization of the axial conformation in substituted cyclohexane originates from the repulsion between the axial group and the two axial H atoms. If the substituent is a relatively nonpolar CH_3 group, the difference between gas- and solution-phase ΔH is probably not large. However, when electron-withdrawing groups such as Cl or polar groups such as OCH_3 are attached to cyclohexane, the axial/equatorial energy difference varies by as much as 0.3 kcal/mol when a $CFCl_3$ solvent is replaced by the more polar $CHFCl_2$ solvent.[47] These effects are very interesting because they involve both an entropic and an enthalpic interaction between the polar molecule and the solvent. The well-known anomeric effect, which refers to the special attraction of electronegative groups in the 2-position with respect to the ether group in tetrahydropyrans (THP, a saturated six-membered cyclic ether), is so strong that the axial orientation becomes dominant.[47] Because the stability of these conformations is influenced by solvent effects, the measurement of gas-phase energies will help shed light on the magnitude of this effect.

In this paper we review what we have learned about these molecules from the analysis of our REMPI spectra. Included in these studies are the effect of laser polarization, the effect of various substituents on the transition origins, and the effect of changing the valve temperature prior to expansion.

Experimental Approach

Figure 1 shows a diagram of the REMPI apparatus. A pulsed valve provides a beam of sample that is skimmed prior to reaching the ionization region ≈7 cm from the nozzle orifice. The sample is seeded in Ar (typically 2−5% sample) at a total pressure of about 600 Torr. Pulsed laser light from either an excimer pumped or Nd:YAG pumped dye laser is used to excite a two-photon transition to the 3s Rydberg state. In most of the

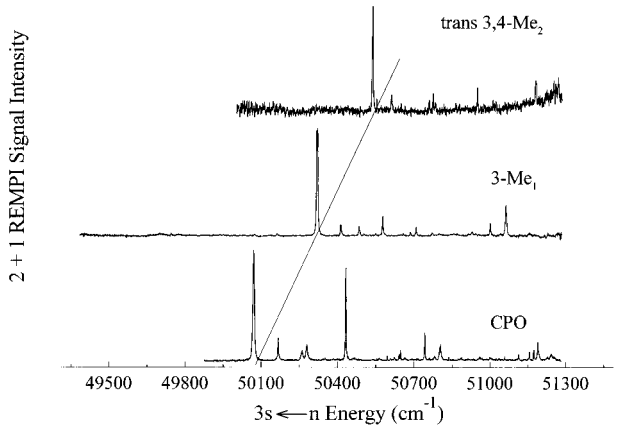

Figure 2. The 2 + 1 REMPI spectra of the 3s ← n transition in cyclopentanone, 3-methylcyclopentanone, and *cis*-3,5-dimethylcyclopentanone. The addition of an equatorial methyl group at the 3-position shifts the origin peak by a constant amount.

molecules investigated, this state lies more than two-thirds of the way toward ionization so that a third photon of the same color can ionize the molecule. Thus, the rate-determining step for ion production is the two-photon absorption, and the ion signal obtained by scanning the laser is a two-photon absorption spectrum of the n → 3s transition ($\sigma \rightarrow$ 3s transition for the case of cyclohexane). The laser is focused by a 25 cm focal length lens at the center of the ionization region. The total electron signal is extracted by applying a 100 V/cm electric field across the two plates of the ionization region. A Stanford Research Systems (SRS) boxcar integrator is used to collect the signal in a 3 ns window. Typical laser powers used are 1−3 mJ/pulse. The laser light is polarized by passing the incident beam through a series of Fresnel rhombs. Two Fresnel rhombs back to back can be angle tuned to change the direction of linear polarization. A third Fresnel rhomb converts the linear polarization to elliptical or circular polarization.

Results and Discussion

Structural Studies of Saturated Ring Compounds by n → 3s Rydberg Spectroscopy. We have investigated the effect of methyl and to a lesser extent ethyl group substitution on five different ring systems and their derivatives.

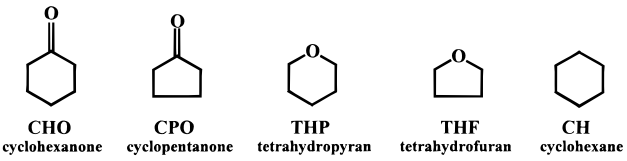

Except in the cases of THF and CH, the dominant peak in the 3s Rydberg transition is the transition origin which shows that there is little geometry change between the molecule in the ground and in the 3s Rydberg state. An example is given in Figure 2 for the case of cyclopentanone (CPO) and two methyl-substituted cyclopentanones (3-MCPO and *trans*-3,4-DMCPO).[40] A strong transition origin is expected for the n → 3s transition since the HOMO has considerable nonbonding character with major contributions from the oxygen lone pairs. Although it is not necessarily expected for cyclohexane because the $\sigma \rightarrow$ 3s transition weakens the C−C σ-bond, the transition origin is nevertheless a strong peak for many of the methyl-substituted cyclohexanes.[41] The tetrahydrofuran spectra are complicated by two features. First, the transition origin is not the dominant peak. Instead, the spectrum is characterized by a long progression in a low-frequency vibration (90 cm^{-1}) which

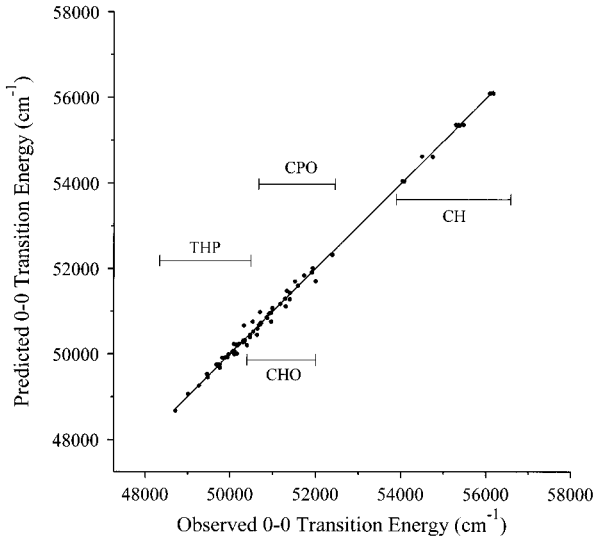

Figure 3. A plot of predicted and measured 3s ← n transition origins for methyl-substituted cyclohexanes, cyclopentanones, cyclohexanones, and tetrahydropyrans. The predicted origins are based on single methyl group shift parameters.

TABLE 1: Average Transition Origin Shifts (in cm^{-1}) for Methyl Substitution in Cyclohexanones and Cyclopentanones

	methyl group position		
	2	3	4
CHO equatorial orientation	−522 ± 15	+124 ± 15	+13 ± 22
CHO axial orientation	−530 ± 35	−446 ± 21	−271 ± 25
CPO equatorial orientation	−308 ± 35	+226 ± 6	
CPO axial orientation	−390 ± 18	−65 ± 71	

can be assigned to a ring deformation mode. This long vibrational progression indicates a significant ring geometry change in the n → 3s transition. Second, a third laser photon is not sufficient to ionize the 3s Rydberg state. Thus, the transition origin can only be reached via a 2 + 2 REMPI transition, thus greatly complicating the spectral analysis. These spectra have not been analyzed in detail.

The interesting aspect of the spectra in Figure 2 is seen in the shifts of the transition origin to the blue. The two methyl groups added at the 3- and 4-positions are both aligned in a pseudoequatorial orientation. They are thus equivalent in the position of substitution and their orientation. We note that the spectral shifts from CPO to 3-MCPO and 3-MCPO to 3,4-DMCPO are nearly equal, +248 cm^{-1} for the first methyl group and an additional +218 cm^{-1} for the second methyl group. The analogous spectra for CPO, 2-MCPO, and *trans*-2,5-DMCPO exhibit red shifts of −369 and −235 cm^{-1}. The shift additivity is not as good as in the 3-position, but still impressive. Similar additivities have been recorded for the other molecules investigated. By collecting spectra for various mono-, di-, and trimethyl compounds, and assuming that the addition of equivalent methyl groups (e.g., axial methyl groups in positions 3 and 5 in cyclohexanone) shifts the transition origins by constant amounts, we were able to derive by least-squares analysis single methyl group shifts. Figure 3 shows the predicted and observed transition origin energies for over 60 methyl-substituted (from monomethyl to tetramethyl) cyclohexane, cyclic ketones, and ethers. In the cyclohexanones and cyclopentanones, methyl group substitution leads to the average shifts shown in Table 1. In the case of tetrahydropyrans, single methyl group shifts range from −746 cm^{-1} (2-axial methyl group) to +411 cm^{-1} (4-equatorial methyl group).

n → 3s Transition Symmetries and Laser Polarization. The effect of the incident light polarization on two-photon

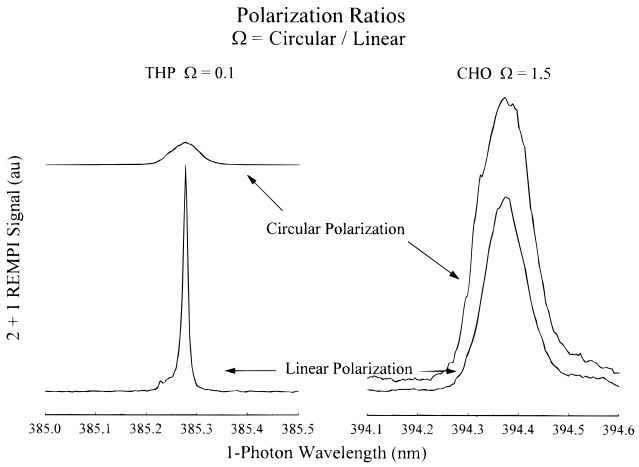

Figure 4. The 2 + 1 REMPI origin band spectra for the 3s ← n transition in cyclohexanone and tetrahydropyran under linear and circular laser polarization.

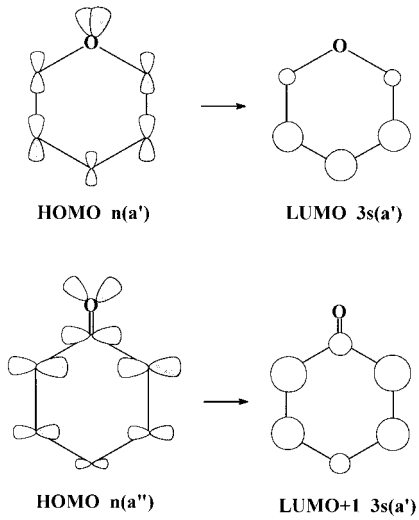

Figure 5. Approximate atomic orbital contributions to the HOMO and LUMO for tetrahydropyran and the HOMO and LUMO + 1 for cyclohexanone. Because the molecules are in nonplanar chair confomations, a number of atomic orbitals at each atom contribute to the molecular orbitals. The size of the p and s atomic orbitals are proportional to their weight in the molecular orbital.

transitions provides some valuable clues about the assignment of the optical transition. The polarization parameter, Ω, is defined as the ratio of peak intensities under circular and linear laser polarization. For rotating symmetric top molecules, the value of Ω can be calculated with the following equation:[48−52]

$$\frac{1}{\Omega} = \frac{2}{3} + \frac{5M_0R_0}{3M_2R_2} \qquad (1)$$

where M_j and R_j are molecular and rotational factors, respectively, in which the subscripts depend on the changes in the rotational quantum number, ΔJ. Normally, $M_0 > M_2$ and $R_0 > R_2$. However, for electronic transitions between states of different symmetry, $M_0 = 0$ so that $\Omega = {}^3/_2$ and is independent of rotational quantum levels. The same ratio is expected for the O, P, R, and S branches in all transitions regardless of symmetry. The Q branch, however, for transitions between states of the same symmetry, in which $M_0 \neq 0$ and $R_0 \neq 0$, deviates from the ${}^3/_2$ value. The resulting value of the polarization ratio is $\Omega < {}^3/_2$.

Figure 4 compares the n → 3s spectra of cyclohexanone and tetrahydropyran under linear and circular polarization of the laser light. In CHO, $\Omega = {}^3/_2$, while in THP, $\Omega < 0.1$. This suggests that the transition in CHO is between different symmetry states, thereby yielding an $M_0 = 0$ and an $\Omega = {}^3/_2$, while the transition in THP is between states of the same symmetry. In both the ketone and the ether ring system, the oxygen lone pair orbitals are part of the highest occupied molecular orbital (HOMO). However, as our ab initio calculations show, this orbital is not localized exclusively at the oxygen atom. Figure 5 shows the contribution of some of the atomic orbitals to the HOMO and the LUMO and LUMO + 1 of THP and CHO, respectively. It is evident that the HOMO is spread over the whole molecule, drawing significant contributions from the carbon p-orbitals, the sizes of which in the figure are approximately proportional to their contribution. The composition of the 3s Rydberg state, i.e., the LUMO virtual orbital in THP and the LUMO + 1 orbital in CHO, also receives contributions from all the carbon atoms in the ring, but in this case the contributing atomic orbital is primarily the 3s orbital. Because of the chair structure, the only symmetry element in THP and CHO is a mirror plane, thus placing these molecules in the C_s symmetry group which yields A′ and A″ states. It is easy to see how the HOMO symmetries of the two molecules differ if we consider the hybridized lone pair orbitals. In the case of THP, the oxygen atom hybridization is sp^3 so that the two lone pair orbitals lie in the perpendicular symmetry plane. The HOMO for THP is thus of a′ symmetry. In the case of CHO, the carbonyl π bond lies in the symmetry plane while the two lone pairs in the sp^2 hybrids lie on either side of the symmetry plane. The HOMO for CHO is thus of a″ symmetry. In both molecules, the 3s Rydberg orbital has a′ symmetry. Because the ground state of both molecules is A′, the n → 3s transitions are between A′ and A′ states for THP and between A′ and A″ states for CHO.

It is apparent that the CHO and THP spectra under linear polarization also differ in their peak widths, a difference that is readily explained by the different transition symmetries. The THP transition origin peak under linear polarization is composed predominantly of Q branch ($\Delta J = 0$) transitions. This branch can be excited by linearly polarized light which contains a mixture of right and left polarized light ($\Delta J = \pm 1$). On the other hand, the much smaller THP peak obtained with circular polarized light ($\Delta J = +1$ or $J = -1$) is composed mostly of S ($\Delta J = +2$) and O ($\Delta J = -2$) branches. The Q branch cannot be excited by two photons with the same angular momentum.

It is interesting to determine whether these symmetry rules which are derived for small and symmetric molecules hold for the molecules under study here. Does methyl substitution far from the nominal C═O chromophore affect the Ω value? The answer seems to be inconsistent. For instance, the symmetric 4-MCHO, *cis*-3,5-DMCHO, and *cis*-2,6-DMCHO all have Ω = 1.5, while the unsymmetric *trans*-3,5-DMCHO has an Ω = 0.90.[34] However, the chiral 3-MCHO and *trans*-3,4-DMCHO have an Ω = 1.5 rather than an expected Ω of 1.0 for nonsymmetric molecules. In the case of the tetrahydropyrans, the situation is even more confusing. For instance, while the symmetric THP, 4-MTHP, and the unsymmetric 2,4-DMTHP have $\Omega \approx 0.08$ as expected for symmetric molecules, the symmetric *cis*-3,5-DMTHP has an Ω = 0.68.[35] The origin of these unexpected Ω values is not understood.

The atomic orbital contributions in Figure 5 show that, for both CHO and THP, the greatest contribution to the 3s wave function comes from the ring carbons and not from the oxygen atom. This may partially explain why these n → 3s transitions are particularly sensitive to the position and orientation of the substituents. Methyl groups would perturb the 3s state of the

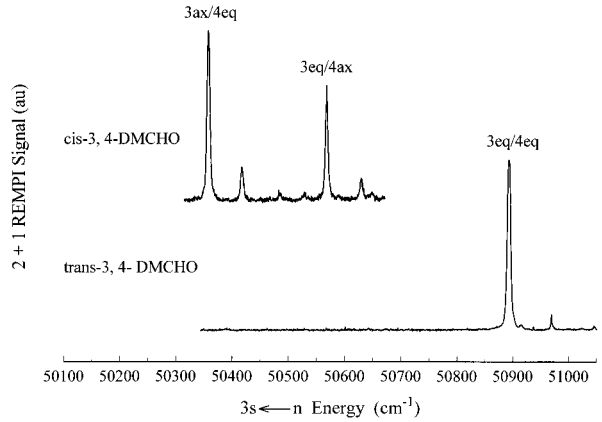

Figure 6. The 2 + 1 REMPI spectra of *cis*-3,4-dimethylcyclohexanone and *trans*-3,4-dimethylcyclohexanone. Note the two conformations for the cis isomer.

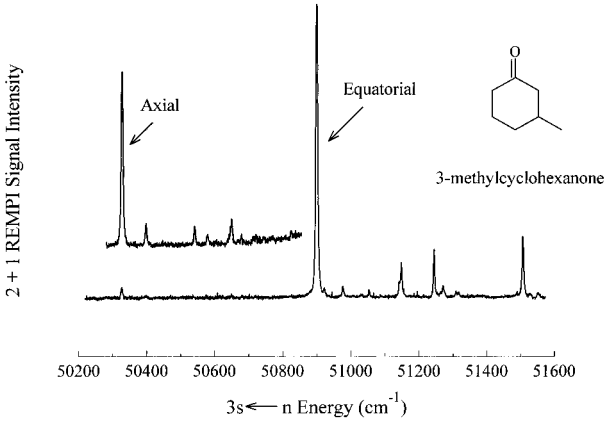

Figure 7. The 2 + 1 REMPI spectrum of 3-methylcyclohexanone. The molecular beam has frozen out the axial methyl group conformer.

carbon atom to which it is bonded, which in turn alters the energy of the 3s molecular Rydberg state.

Cooling and Trapping of Conformations in a Molecular Beam. So far, we have considered only the spectra of configurational isomers, such as *cis*- and *trans*-3,4-DMCHO (see Figure 6). These are different molecules and can thus be physically separated. However, it is also possible to trap rapidly interconverting conformations by cooling them in the molecular beam. The *trans*-3,4-DMCHO molecule is most stable when both methyl groups are in their equatorial orientation. The alternate conformation with both methyl groups oriented axially is much too unstable to be observed in the spectrum. However, consider now the *cis*-3,4-DMCHO molecule (also shown in Figure 6) which can exist in either the 3-axial-4-equatorial or 3-equatorial-4-axial conformation. The energies of the two conformers are nearly equal which is reflected in the similar peak intensities. What about their expected transition origins? According to Table 1, the 3-axial-4-equatorial conformation has a predicted shift, relative to unsubstituted CHO, of $-446 + 13 = -433$ cm^{-1}, while the 3-equatorial-4-axial conformation has a predicted shift of $+124 - 271 = -147$ cm^{-1}. Experimentally, we find them to have shifts of -396 and -177 cm^{-1}, respectively. Thus, these two conformational isomers can be easily distinguished by their transition origins. Similarly, any of the monomethyl compounds can exist in either the axial or equatorial conformation. Figure 7 shows the spectrum of 3-MCHO in which the red-shifted axial conformer shows up at 50 297 cm^{-1}, which is close to the predicted origin of 50 271 cm^{-1}. Unlike the two nearly equal energy *cis*-3,4-DMCHO conformers which appear with nearly equal intensity, the axial

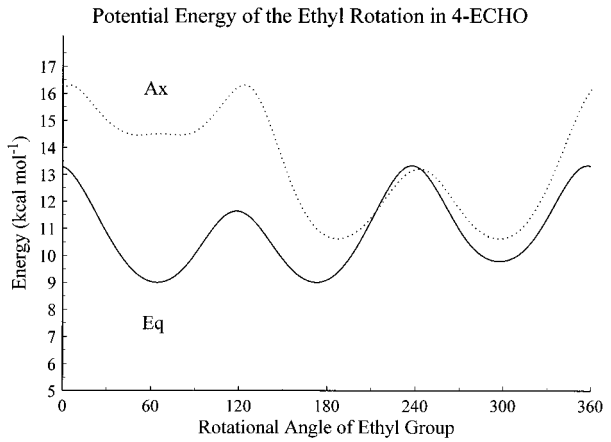

Figure 8. The potential energy surface calculated by molecular mechanics of the ethyl rotor in the axial and equatorial orientation of 4-ethylcyclohexanone.

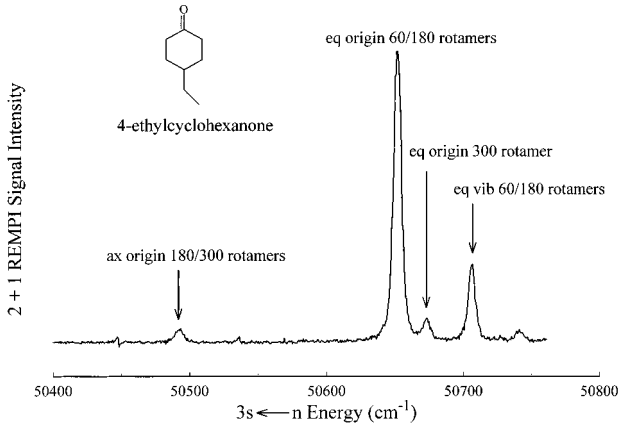

Figure 9. The 2 + 1 REMPI spectrum of 4-ethylcyclohexanone. The various ethyl rotor orientations are indicated.

3-MCHO peak is only 5% of the equatorial 3-MCHO peak, thereby reflecting the much lower population of this conformer in the molecular beam. The spectra of nearly all of the methyl-substituted cyclohexanones and tetrahydropyrans show peaks assignable to multiple conformers. The only exception is the 2-MCHO in which only the more stable equatorial conformation is evident. A similar absence of higher energy conformations was noted for the methyl-substituted cyclopentanones.

Ethyl Group Rotors in Ethyl Cyclohexanones and Ethyl Cyclopentanones. The substitution of an ethyl group adds additional degrees of freedom, namely the ethyl group rotation. There are six ethyl rotor conformations. Figure 8 shows a molecular mechanics diagram of the three stable rotamers with the ethyl group equatorial and three with the ethyl group axial for 4-ECHO. A plane of symmetry in this molecule dictates that two of the three rotamers are degenerate. The rotamers are distinguished by their dihedral angle with the ring. So equatorial 60/180 are degenerate, and equatorial 300 is the rotamer with the ethyl group in the symmetric ring plane. A chair−chair flip results in the axial conformer where the axial 180/300 are degenerate rotamers. The n → 3s spectrum of 4-ECHO in Figure 9 now shows three peaks which can be identified on the basis of their intensities and their position.[29] As in the case of the 3-MCHO in Figure 7, the axial conformer is significantly red-shifted. Thus, the small peak at 50 490 cm^{-1} is readily identified with the degenerate axial conformer that is significantly populated at room temperature. The large peak at 50 650 cm^{-1} can be identified with the most stable equatorial rotamer (the degenerate rotor orientation). Finally, the small

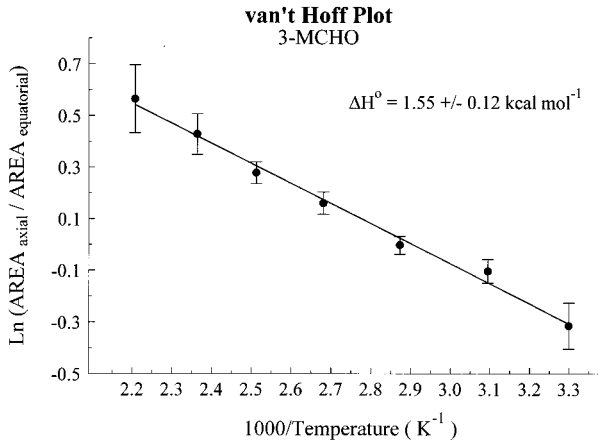

Figure 10. The van't Hoff plot for the 3-methylcyclohexanone axial−equatorial equilibrium.

peak to the red of the large one is the correct intensity to be identified with the equatorial 300 rotor position in which the ethyl group is in the molecule's symmetry plane. The peak to the blue which is identified as a vibrationally excited state of the equatorial 60/180 rotamer was identified by analogy with the 4-MCHO and also its intensity variation when the valve temperature was increased (next section). The peak intensities have been quantitatively identified by their intensities for 2-, 3-, and 4-ECHO and 2- and 3-ECPO.[29] Under the assumption that these conformations are frozen out in the molecular beam at their 298 K populations (the sudden freeze assumption), their population in the molecular beam can be calculated by using energies based on either molecular mechanics or ab initio MO (with corrections for zero-point energies) methods. This approach worked extremely well for all the molecules investigated, which lends strong support for the sudden freeze assumption.

Temperature-Dependent Spectra of Cyclic Ketones and Heats of Isomerization. In the spectral analysis of the axial and equatorial methyl conformations as well as in the ethyl rotor conformations, it was suggested that spectral peak areas could be related to the populations of the various conformers. Two assumptions are implied in this comparison. First, we assume that the ratios of the origin peak intensities for the various conformations are identical to the ratio of the integrated peak intensity of the entire electronic band. Second, it is assumed that the REMPI signals are directly related to the absorption cross section. Because the REMPI signal depends upon the lifetime of the intermediate 3s Rydberg state, and because this state can be depleted by nonradiative processes such as internal conversion or dissociation, it is not obvious that the REMPI signals for different conformations can be related to concentrations. For these reasons, it was desirable to carry out experiments in which the pulsed valve temperature was varied so that the ΔH between axial and equatorial conformations could be determined through the van't Hoff equation.

$$\ln \frac{K(T_2)}{K(T_1)} = -\frac{\Delta H}{R}\left(\frac{1}{T_2} - \frac{1}{T_1}\right) \qquad (2)$$

The advantage of this approach is that the derived ΔH depends only on the *ratio* of equilibrium constants so that factors other than concentration that determine spectral intensities for the axial and equatorial conformations will cancel.

The results for the 3-MCHO are shown in Figure 10 in which the temperature was varied from 30 to 180 °C.[43] The slope yields an enthalpy of 1.55 ± 0.12 kcal/mol. One of the critical questions is whether the sudden freeze assumption is correct.

TABLE 2: Calculated and Measured Axial/Equatorial Enthalpy Differences (kcal/mol) of Four Substituted Cyclohexanones

	3-MCHO	4-MCHO	*cis*-3,4-DMCH	*cis*-2-decalone
gas-phase REMPI (this work)	1.55 ± 0.12[a]	2.1 ± 0.20	0.33 ± 0.10	0.43 ± 0.06
epimerization GLC	1.30,[b] 1.36[c]			
NMR	1.1[d]	1.1[e]; 1.9[f]	0.50[g]	0.23,[h] −0.12[i]
MM2	1.40[a]	1.67	0.22	0.26
MM3	1.57[j]	1.87[j]	0.20[j]	0.28[j]
HF/6-31G*	1.77[a]	2.21	0.37	0.40
G2(MP2)	1.03[a]	1.43		
B3LYP/6-31G*	1.65[a]	2.00	0.34	0.33

[a] Reference 43. [b] Reference 85. [c] Reference 53. [d] Reference 86. [e] Reference 86. [f] Reference 87. [g] Reference 88. [h] Reference 60. [i] Reference 62. [j] Courtesy of N. L. Allinger. (The PC version of MM3[59] is not yet available.)

The fact that the van't Hoff plot shows no curvature at high temperatures suggests that it is correct. If the axial/equatorial equilibrium had time to adjust, then one would expect a leveling off in the van't Hoff plot at high temperatures. This is not evident. Second, any cooling of the equilibrium concentrations would tend to reduce the slope. Since our slope yields a value for $\Delta H°$ which is higher than other experiments (see Table 2), all the indications are that the sudden freeze assumption is justified in this case.

The measured $\Delta H°$ for the axial/equatorial equilibrium for 3-MCHO is the first reliable direct measurement of this quantity. Previous studies relied on epimerization methods in which 2,5- and 3,5-dimethylcyclohexanones were catalytically equilibrated, and the ratios of cis and trans isomers were measured by gas−liquid chromatography.[53] The assumption in this approach was that the second methyl group has no effect on the methyl group in the 3-position. These studies yielded $\Delta H°$ values of 1.30 and 1.36 kcal/mol, respectively. Other studies based on ultrasound relaxation methods gave rather scattered values from 0.6 to 2.8 kcal/mol.[54,55] It is important to point out that our values refer to the gas-phase equilibrium, whereas all other measurements were done in solution.

It is interesting that our measured values are consistently higher than those calculated by the MM2 program.[56] In the case of the 4-methylcyclohexanone, the difference is more than 0.4 kcal/mol. The more recent molecular mechanics parametrization, MM3,[57−59] does considerably better but still appears a bit low for 4-MCHO.

Our efforts to calculate the enthalpy difference by ab initio MO methods yielded mixed results as shown in Table 2.[44] The Hartree−Fock method (HF/6-31G*) is in good agreement with the experiment. It is noteworthy that inclusion of correlation [HF/6-31G*/MP2 or G2(MP2)] made the agreement worse. In addition, we have found that density functional methods, especially with the Lee, Yang, Parr functional, provide accurate ΔH values at a fraction of the computer time necessary to do the G2(MP2) calculation. The G2 calculation for 3-methylcyclohexanone required between 30 and 40 h of CRAY time per conformation compared to less than 10 h for the density functional theory calculation.

Decalone is an interesting bicyclic ketone in which a cyclohexanone ring is fused to a cyclohexane ring. When the cyclohexane ring is connected at the 3- and 4-positions of the cyclohexanone, and they are connected in a cis configuration, the decalone is a basic unit of all steroids. Figure 11 shows the spectrum of *cis*-2-decalone. The trans configuration is diequatorial, and thus only a single peak conformation is evident. However, the cis configuration can be either 3eq/4ax (the

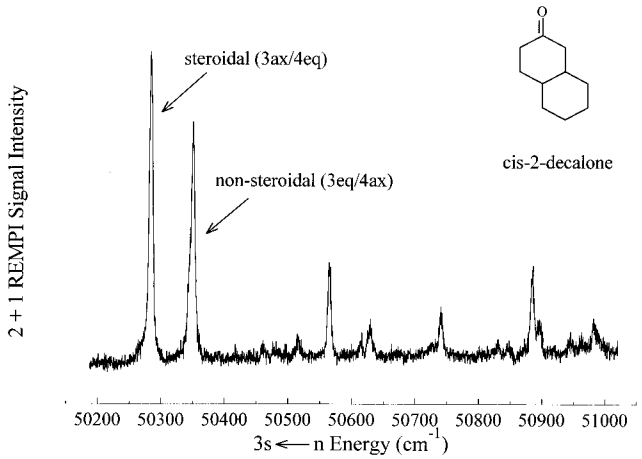

Figure 11. The 2 + 1 REMPI spectrum of *cis*-2-decalone. The two large peaks correspond to two different conformations.

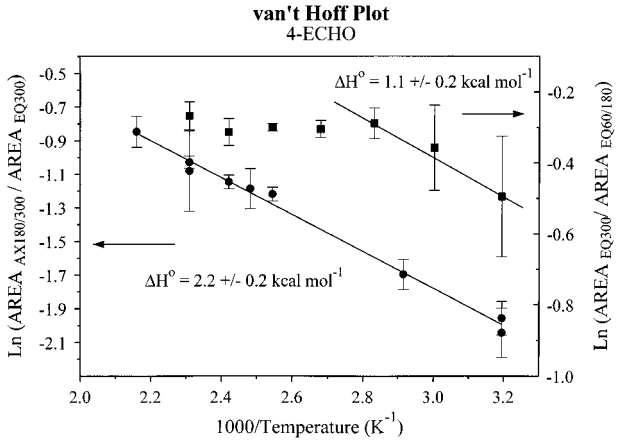

Figure 12. The van't Hoff plot for two equilibria of 4-ethylcyclohexanone. On the left is the axial−equatorial equilibrium and on the right is the ethyl rotor equilibrium.

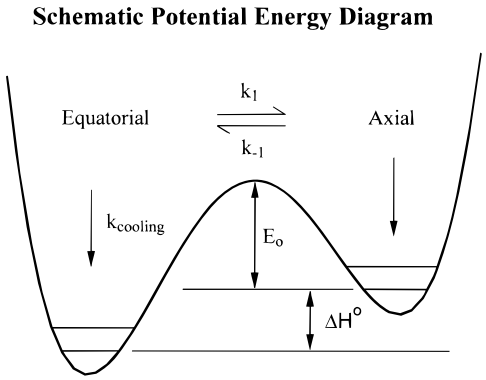

Figure 13. A model of the potential energy surface for the axial−equatorial equilibration obtained by molecular mechanics.

steroidal form) or 3ax/4eq (the nonsteroidal form). The larger of the two peaks in the spectrum is due to the nonsteroidal 3ax/4eq conformation. This is as expected since according to Table 2, the $\Delta H°$ for the axial−equatorial equilibrium in 3-MCHO is less than in 4-MCHO. This is due to the well-known 3-alkyl ketone effect in which the ketone group stabilizes the axial methyl group in the 3-position.[46]

A variable temperature study of *cis*-2-decalone between 323 and 473 K produced a linear van't Hoff plot, the slope of which yielded a $\Delta H°$ of 0.43 ± 0.06 kcal/mol, which is somewhat larger than that obtained for the related 3,4-dimethyl-CHO equilibrium (see Table 2). We do not know yet whether this is because the cyclohexane ring prohibits the 3ax/4eq conformer from minimizing its energy or whether it is simply the larger alkyl group in the decalone relative to the DMCHO that destabilizes this conformation. Investigation of the 3,4 diethyl-CHO may provide the answer.

There are three reports of experimental conformational $\Delta G°$'s for 2-decalone.[60−62] Two independent experiments were performed using low-temperature NMR, and the $\Delta G°$'s are 0.23 kcal mol^{-1} at 186 K and 0.21 kcal mol^{-1} at 203 K. The only room-temperature literature value was obtained using lanthanide-induced shift reagents, LIS(NMR). From this study it was determined that the 3eq/4ax steroidal form was the more stable conformer by 0.12 kcal mol^{-1} at 298 K. This contradicts both the low-temperature results and our REMPI result. Our ab initio MO calculations of the two decalone conformations provided a set of vibrational frequencies from which we could calculate a $\Delta S° = -0.05$ cal/(mol K) at 298 K. Thus, the ΔG and ΔH values differ by only 0.015 kcal/mol at room temperature. This difference is not enough to explain the discrepancy between our REMPI ΔH value and the low-temperature NMR ΔG value.

The Ethyl Rotor Equilibration. As the spectrum in Figure 9 illustrates, the molecular beam freezes out two equatorial conformations of the ethyl rotor in 4-ECHO as well as one axial conformation.[29] An axial/equatorial flip converts the axial conformation into the most stable rotor orientation of the equatorial conformation. It is thus possible to generate a van't Hoff plot for both equilibria. These are shown in Figure 12.[63] As in 3- and 4-MCHO, the van't Hoff plot for the axial−equatorial equilibrium for the 4-ethyl CHO is linear up to the highest temperatures investigated. However, the van't Hoff plot for the ethyl rotor equilibration within the equatorial conformation is linear only up to 80 °C. Above this temperature, the isomerization reaction apparently is more rapid than vibrational relaxation. The competition between the unimolecular isomerization and collisional vibrational relaxation rates is shown schematically in Figure 13.

The trapping of isomeric forms in supersonic expansions has been noted by numerous workers.[12−27] Ruoff et al.[15] have suggested a criterion for the observation of higher energy isomers which is that isomers separated by barriers in excess of 1 kcal/mol should freeze out. However, this criterion, based on experiments with several sets of van der Waals dimer isomers, is severely limited. It does not take into account the dynamics of vibrational relaxation or the nature of the isomerization reaction.

The break in the van't Hoff plot for the ethyl rotor may provide us with a means for investigating the cooling of molecules in molecular beams. It may be possible to use a calculated rotamer equilibration rate from transition-state theory to model the collisional vibrational relaxation rate as a function of the distance from the nozzle orifice. Translational temperatures and gas density variations in nozzle expansions of samples highly diluted in rare gases are fairly well established.[64−66] The missing element for a full understanding is the collisional vibrational relaxation rates, especially at low temperatures. Although, dramatic advances have been made in our understanding of vibrational energy-transfer processes in large molecules,[67−73] these studies have been devoted primarily to highly excited species. They have yielded collisional energy transfer probability function, $P(E,E')$, which is the probability (per collision event) of energy transfer from E' to E. It has been found that as long as the general form of the $P(E,E')$ function is correct, minor details are not important. A commonly used form is the exponential down transition, which describes the process by a single parameter, e.g., the average

energy transfer per collision,[74] which is a function of the total energy. The upward transitions are related to the down transitions by detailed balance. The energy transfer probability or ΔE decreases with total energy.

At the present time, $P(E,E')$ functions are not known for polyatomic molecules at low temperatures. However, it should be possible to generate a one- or two-parameter $P(E,E')$ function which can be used along with the calculated unimolecular isomerization rates in a solution of the master equation[75−78] which in its integral form is given by

$$dN(E)/dt = \omega \int_0^\infty [P(E,E')\, N(E') - P(E',E)\, N(E)]\, dE' - k(E)\, N(E) \quad (3)$$

where ω is the hard-sphere collision frequency, $N(E)$ is the population of molecules with an internal energy, E, and $k(E)$ is the unimolecular reaction rate for a molecule with energy E. The solution of this master equation yields the final population of the conformers in the cold molecular beam. The parameters in the $P(E,E')$ function can be varied until the break in the van't Hoff plot for the ethyl rotor is reproduced. The experimental variables are the initial pressure of the gas in the nozzle and the nature of the diluent gas. The final vibrational temperature of the sample can also be modeled by reducing the backing gas pressure or replacing the more efficient Ar cooling gas with He. The observation of hot bands can then be modeled with the same master equation. Plans for such studies are in progress.[79]

Conclusions

We have found that the n → 3s Rydberg spectra of cyclohexane and a series of oxygen-containing ring systems are extremely sensitive to subtle changes in molecular conformation. Large shifts in the transition origins are observed when alkyl groups are substituted at various locations on the ring. The magnitude and sign of the shifts are characteristic of the substituent position as well as its orientation. This makes the n → 3s REMPI spectroscopy an ideal tool for the investigation of conformational equilibria. By varying the temperature of the pulsed nozzle, we have demonstrated for a number of molecules that vibrational relaxation is much more rapid than conformational equilibration. Thus, the "sudden freeze" model is appropriate even though the interconversion barriers for the axial−equatorial reaction in cyclohexanone is only 4−5 kcal/mol.

Can this type of spectroscopy be applied to other molecular systems? Preliminary investigations on open-chain ketones and ethers such as butanone and diethyl ether[80] indicate that strong n → 3s REMPI signals are readily obtainable. In addition, strong and sharp signals are obtained for many bicyclic compounds such as verbanone, nopinone, and camphor.[81] Finally, tetrahydrothiophene and pyridine have good spectra. However, we have also found that substitution of some groups such as OH or the insertion of double bonds in the ring results in the loss of the REMPI signal. The cause of this could be rapid dissociation of the intermediate state prior to absorption of the third photon. Or, perhaps, a rapid internal conversion to the ground electronic state causes the signal to disappear. In either case, replacing the nanosecond laser with a picosecond laser might help overcome this problem. Pulse widths shorter than picoseconds are not useful for spectroscopic purposes because the laser bandwidth becomes too broad.

Although the spectral sensitivity to structural properties has been useful in deriving interesting information about the energetics of saturated cyclic systems, we have not been successful in understanding the origin of this remarkable sensitivity. We have found that the REMPI shifts are related to C-13 carbonyl shifts[38,40] and that these shifts are perhaps related to ground-state van der Waals interactions.[82−84] But so far a global understanding of the shift origins has been elusive.

Acknowledgment. We thank N. L. Allinger and Kuo-Hsiang Chen of the University of Georgia for providing us with MM3 calculations. We also thank the National Science Foundation for support of this work.

References and Notes

(1) Laane, J. In *Vibrational Spectra and Structure;* Durig, J. R., Ed.; Marcel Dekker: New York, 1972; p 26.
(2) Ikeda, T.; Lord, R. C. *J. Chem. Phys.* **1972**, *56*, 4450.
(3) Rosas, R. L.; Cooper, C.; Laane, J. *J. Phys. Chem.* **1990**, *94*, 1830.
(4) Cadioli, B.; Gallinella, E.; Coulombeau, C.; Jobic, H.; Berthier, G. *J. Phys. Chem.* **1993**, *97*, 7844.
(5) Cui, W.; Li, F.; Allinger, N. L. *J. Am. Chem. Soc.* **1993**, *115*, 2943.
(6) Bernard, M.; Canuel, L.; St-Jacques, M. *J. Am. Chem. Soc.* **1974**, *96*, 2929.
(7) Anet, F. A. L.; Chmurny, G. N.; Krane, J. *J. Am. Chem. Soc.* **1973**, *95*, 4423.
(8) Levy, D. H. *Annu. Rev. Phys. Chem.* **1980**, *31*, 197.
(9) Lubman, D. M. *Anal. Chem.* **1987**, *59*, 31A.
(10) Johnson, P. M. *Acc. Chem. Res* **1980**, *13*, 20.
(11) Hayes, J. M. *Chem. Rev. (Washington, D.C.)* **1987**, *87*, 745.
(12) Miller, R. E. *Science* **1988**, *240*, 447.
(13) Block, P. A.; Jucks, K. W.; Pedersen, L. G.; Miller, R. E. *Chem. Phys.* **1989**, *139*, 15.
(14) Dayton, D. C.; Pedersen, L. G.; Miller, R. E. *J. Phys. Chem.* **1992**, *96*, 1087.
(15) Ruoff, R. S.; Klots, T. D.; Emilsson, T.; Gutowsky, H. S. *J. Chem. Phys.* **1990**, *93*, 3142.
(16) Klots, T. D.; Ruoff, R. S.; Gutowsky, H. S. *J. Chem. Phys.* **1989**, *90*, 4217.
(17) Breen, P. J.; Bernstein, E. R.; Seeman, J. I.; Secor, H. V. *J. Phys. Chem.* **1989**, *93*, 6731.
(18) Seeman, J. I.; Secor, H. V.; Disselkamp, R.; Bernstein, E. R. *J. Chem. Soc., Chem. Commun.* **1992**, 713.
(19) Breen, P. J.; Warren, J. A.; Bernstein, E. R.; Seeman, J. I. *J. Chem. Phys.* **1987**, *87*, 1927.
(20) Seeman, J. I.; Paine, J. B.; Secor, H. V.; Im, H. S.; Bernstein, E. R. *J. Am. Chem. Soc.* **1992**, *114*, 5269.
(21) Li, S.; Bernstein, E. R.; Secor, H. V.; Seeman, J. I. *Tetrahedron Lett.* **1991**, *32*, 3945.
(22) Martinez, S. J.; Alfano, J. C.; Levy, D. H. *J. Mol. Spectrosc.* **1992**, *152*, 80.
(23) Cable, J. R.; Tubergen, M. J.; Levy, D. H. *Faraday Discuss. Chem. Soc.* **1988**, *86*, 143.
(24) Finley, J. P.; Cable, J. R. *J. Phys. Chem.* **1994**, *98*, 3950.
(25) Buma, W. J.; Kohler, B. E.; Song, K. *J. Chem. Phys.* **1991**, *94*, 4691.
(26) Ci, X.; Kohler, B. E.; Shaler, T. A.; Moller, S.; Yee, W. A. *J. Phys. Chem.* **1993**, *97*, 1515.
(27) Felder, P.; Gunthard, H. H. *Chem. Phys.* **1982**, *71*, 9.
(28) Driscoll, J. W.; Baer, T.; Cornish, T. J. *J. Mol. Struct.* (*THEOCHEM*)-**1991**, *249*, 95.
(29) Nesselrodt, D. R.; Potts, A. R.; Baer, T. *J. Phys. Chem.* **1995**, *99*, 4458.
(30) Im, H. S.; Bernstein, E. R.; Secor, H. V.; Seeman, J. I. *J. Am. Chem. Soc.* **1991**, *113*, 4422.
(31) Tubergen, M. J.; Cable, J. R.; Levy, D. H. *J. Chem. Phys.* **1990**, *92*, 51.
(32) Martinez, S. J.; Alfano, J. C.; Levy, D. H. *J. Mol. Spectrosc.* **1993**, *158*, 82.
(33) Cornish, T. J.; Baer, T. *J. Am. Chem. Soc.* **1987**, *109*, 6915.
(34) Cornish, T. J.; Baer, T. *J. Am. Chem. Soc.* **1988**, *110*, 3099.
(35) Cornish, T. J.; Baer, T. *Anal. Chem.* **1990**, *62*, 1623.
(36) Cornish, T. J.; Baer, T.; Pedersen, L. G. *J. Phys. Chem.* **1989**, *93*, 6064.
(37) Cornish, T. J.; Baer, T. *J. Phys. Chem.* **1990**, *94*, 2852.
(38) Cornish, T. J.; Baer, T. *J. Am. Chem. Soc.* **1988**, *110*, 6287.
(39) Nesselrodt, D. R.; Baer, T. *Anal. Chem.* **1994**, *66*, 2497.
(40) Potts, A. R.; Nesselrodt, D. R.; Baer, T.; Driscoll, J. W.; Bays, J. P. *J. Phys. Chem.* **1995**, *99*, 12090.
(41) Nesselrodt, D. R.; Potts, A. R.; Baer, T. *Anal. Chem.* **1995**, *67*, 4322.
(42) Nesselrodt, D. R.; Baer, T. *J. Mol. Spectrosc.* **1996**, *377*, 201.
(43) Potts, A. R.; Baer, T. *J. Chem. Phys.* **1996**, *105*, 7605.
(44) Potts, A. R.; Baer, T. *J. Mol. Struct. (THEOCHEM),* in press.

(45) Driscoll, J. W.; Baer, T. *Anal. Chem.* **1992**, *64*, 2604.
(46) Eliel, E. L.; Wilen, S. H. *Stereochemistry of Organic Compounds*; John Wiley & Sons: New York, 1994.
(47) Booth, H.; Khedhair, K. A.; Readshaw, S. A. *Tetrahedron* **1987**, *43*, 4699.
(48) Pechukas, P. *J. Chem. Phys.* **1976**, *64*, 1516.
(49) Nascimento, M. A. C. *Chem. Phys.* **1983**, *74*, 51.
(50) Monson, P. R.; McClain, W. M. *J. Chem. Phys.* **1970**, *53*, 29.
(51) Lin, S. H.; Fujimura, Y.; Neusser, H. J.; Schlag, E. W. *Multiphoton Spectroscopy of Molecules*; Academic Press: Orlando, FL, 1984.
(52) Wirth, M. J.; Koskelo, A.; Sanders, M. J. *Appl. Spectrosc.* **1981**, *35*, 14.
(53) Allinger, N. L.; Freiberg, L. A. *J. Am. Chem. Soc.* **1962**, *84*, 2201.
(54) Heywood, P. J.; Rassing, J. E.; Wyn-Jones, E. *Adv. Mol. Relax. Proc.* **1975**, *6*, 307.
(55) Reddy, B. A.; Rao, N. P. *Can. J. Chem.* **1981**, *59*, 3084.
(56) Burkert, U.; Allinger, N. L. *Molecular Mechanics*; American Chemical Society: Washington, DC, 1982.
(57) Allinger, N. L.; Yuh, Y. H.; Lii, J.-H. *J. Am. Chem. Soc.* **1989**, *111*, 8551.
(58) Lii, J.-H.; Allinger, N. L. *J. Am. Chem. Soc.* **1989**, *111*, 8566.
(59) Allinger, N. L.; Chen, K.; Rahman, C. M.; Pathiaseril, A. *J. Am. Chem. Soc.* **1991**, *113*, 4505.
(60) Abraham, R. J.; Bergen, H. A.; Chadwick, D. J. *Tetrahedron* **1982**, *38*, 3271.
(61) Pehk, T.; Laht, A.; Lippmaa, E. *Org. Magn. Reson.* **1982**, *19*, 21.
(62) Browne, L. M.; Klinck, R. E.; Strothers, J. B. *Org. Magn. Reson.* **1979**, *12*, 561.
(63) Potts, A. R.; Baer, T. *J. Chem. Phys.*, in press.
(64) Miller, D. R. In *Atomic and Molecular Beam Methods;* Scoles, G., Ed.; Oxford University Press: New York, 1988; p 14.
(65) Anderson, J. B.; Andres, R. P.; Fenn, J. B. *Adv. Chem. Phys.* **1966**, *10*, 275.
(66) DePaul, S.; Pullman, D.; Friedrich, B. *J. Phys. Chem.* **1993**, *97*, 2167.
(67) Barker, J. R.; Brenner, J. D.; Toselli, B. M. *Adv. Chem. Kinet. Dyn.* **1995**, *2B*, 393.
(68) Forst, W. *Adv. Chem. Kinet. Dyn.* **1995**, *2B*, 427.
(69) Mullin, A. S.; Michaels, C. A.; Flynn, G. W. *J. Chem. Phys.* **1995**, *102*, 6032.
(70) Flynn, G. W.; Parmenter, C. S.; Wodtke, A. M. *J. Phys. Chem.* **1996**, *100*, 12817.
(71) Michaels, C. A.; Flynn, G. W. *J. Chem. Phys.* **1997**, *106*, 3558.
(72) Hartland, G. V.; Qin, D.; Dai, H. L. *J. Chem. Phys.* **1994**, *100*, 7832.
(73) Hartland, G. V.; Qin, D.; Dai, H. L. *J. Chem. Phys.* **1995**, *102*, 8677.
(74) Penner, A. P.; Forst, W. *J. Chem. Phys.* **1977**, *67*, 5296.
(75) Gilbert, R. G.; Smith, S. C. *Theory of Unimolecular and Recombination Reactions*; Blackwell Scientific: Oxford, 1990.
(76) Bedanov, V. M.; Tsang, W.; Zachariah, M. R. *J. Phys. Chem.* **1995**, *99*, 11452.
(77) Green, N. J. B.; Marchant, P. J.; Perona, M. J.; Pilling, M. J.; Robertson, S. H. *J. Chem. Phys.* **1992**, *96*, 5896.
(78) Tsang, W.; Bedanov, V. M.; Zachariah, M. R. *J. Phys. Chem.* **1996**, *100*, 4011.
(79) Tsang, W.; Baer, T.; Potts, A. R. Unpublished results, 1997.
(80) Shang, Q. Y.; Moreno, P. O.; Disselkamp, R.; Bernstein, E. R. *J. Chem. Phys.* **1993**, *98*, 3703.
(81) Driscoll J. W. Structural and Conformational Analysis of Heterocyclic Organic Compounds Using Resonance Enhanced Multi-photon Ionization. Ph.D. Thesis, University Microfilms, Ann Arbor, MI, 1993.
(82) Li, S.; Chesnut, D. B. *Magn. Reson. Chem.* **1985**, *23*, 625.
(83) Li, S.; Chesnut, D. B. *Magn. Reson. Chem.* **1986**, *24*, 93.
(84) Chesnut, D. B.; Wright, D. W.; Krizek, B. A. *J. Mol. Spectrosc.* **1988**, *190*, 99.
(85) Cotterill, W. D.; Robinson, M. J. T. *Tetrahedron* **1964**, *20*, 777.
(86) Abraham, R. J.; Chadwick, D. J.; Griffiths, L.; Sancassan, F. *J. Am. Chem. Soc.* **1980**, *102*, 5128.
(87) Cotterill, W. D.; Robinson, M. J. T. *Tetrahedron* **1964**, *20*, 765.
(88) Pons, A.; Chapat, J. P. *Tetrahedron* **1980**, *36*, 2297.